

Madras IMSc-91/33

IISc-CTS 7/91

February 12, 2004

Three Dimensional Chern-Simons Theory as a Theory of Knots and Links

R.K. Kaul*

Centre for Theoretical Studies, Indian Institute of Science

Bangalore 560 012, India

and

T.R.Govindarajan†

The Institute of Mathematical Sciences

C.I.T. Campus, Taramani, Madras 600 113, India

Abstract

Three dimensional $SU(2)$ Chern-Simons theory has been studied as a topological field theory to provide a field theoretic description of knots and links in three dimensions. A systematic method has been developed to obtain the link-invariants within this field theoretic framework. The monodromy properties of the correlators of the associated Wess-Zumino $SU(2)_k$ conformal field theory on a two-dimensional sphere prove to be useful tools. The method is simple enough to yield a whole variety of new knot invariants of which the Jones polynomials are the simplest example.

e-mail

*: kaul@vigyan.ernet.in

†: trg@imsc.ernet.in

1. Introduction

Topological quantum field theories have attracted a good deal of interest in recent years. This started particularly with the field theoretic interpretations of two important developments in mathematics: Donaldson's theory for the integer invariants of smooth 4-manifolds in terms of the moduli spaces of $SU(2)$ -instantons¹ and Jones work on knots in three dimensions². These were developed by Witten some years ago^{3,4}. Cohomological field theories involving monopoles of the three dimensions have also been developed.⁵

These applications of topological quantum field theories reflect the enormous interest at present in building a link between quantum physics on one hand and geometry and topology of low dimensional manifolds on the other. It appears that the properties of low dimensional manifolds can be very successfully unravelled by relating them to infinite dimensional manifolds of the fields. This is done through the functional integral formulation of the such quantum field theories. In fact an axiomatic formulation of topological quantum field theories has already been developed by Atiyah⁶. This relates the functional integrals of quantum field theory with of the notion of modular functors.

Witten in his pioneering work⁴ has demonstrated that Jones polynomials of the knot theory are the expectation values of the Wilson loop-operators in a three dimensional $SU(2)$ Chern-Simons theory where the fundamental representation of the gauge group $SU(2)$ lives on the knots. The two variable generalization⁷ of the Jones knot invariants are obtained as the expectation values of the Wilson loop operators with N -dimensional representation living on the knots in an $SU(N)$ Chern-Simons theory. The most important import of the Witten's formulation of the knot theory is that it provides an intrinsically three dimensional description of knots and links. This field theoretic formulation is also powerful enough to study knots and links in any arbitrary three-manifold.

The knot invariants have also been studied from the point of view of exactly solvable models in statistical mechanics^{8,9,10}. The intimate connection that knot invariants have with the exactly solvable lattice models has been exploited by Akutsu, Deguchi and Wadati to obtain a general method for constructing invariant polynomials for knots and links. The Yang-Baxter relation is an important tool in this development. These authors in particular have derived explicitly new knot invariants from a three-state exactly solvable model. These new invariants (both one variable and their two variable generalizations) are indeed more powerful than the Jones polynomials (and their two-variable generalizations).

The knot invariants have also been studied from the quantum group point of view^{11,12}. All these have an intimate connection with two dimensional conformal field theory¹³.

In this paper, following Witten, we shall study the knot theory in terms of a topological quantum field theory. The link invariants are given by the expectation value of Wilson link-operators in a Chern-Simons theory⁴. For definiteness we shall restrict ourselves to the $SU(2)$ gauge group. Generalizations to other groups are straight forward and will be discussed elsewhere. By placing other than the doublet representation of $SU(2)$ on all the component knots of a link we obtain link invariants other than those of Jones. In particular, a triplet representation on all the component knots leads to the one-variable invariants of Akutsu, Deguchi and Wadati obtained from the three state exactly solvable model¹⁰. These invariants obey generalized Alexander-Conway skein relations containing $n + 2$ elements where n is the number of the boxes in the Young tableaux corresponding to the representation that lives on the knots. For $n = 1$, these relations are the standard Alexander-Conway skein relations that relate Jones one-variable polynomials. These were obtained within the field theoretic framework by Witten in ref.[4]. This construction of

Witten can be extended to exhibit the generalized Alexander-Conway skein relations too. After presenting a brief discussion of the non-Abelian Chern-Simons theory in Section 2, we shall present a short derivation of the generalised skein relations in Section 3. These have also been obtained in ref.[14]. While these relations for $n = 1$ case (Jones polynomials) can be recursively solved to obtain Jones polynomials for any knot or link, those for $n \neq 1$ do not contain enough information to allow us to obtain the new invariants for any arbitrary knot or link. Therefore, there is need to develop methods to obtain these invariants. This is what we attempt to do in this paper. In Section 4, we shall present two new types of recursion relations for links for arbitrary n . In Section 5, invariants for links obtained as the closures of braids with two strands, both parallelly oriented and anti-parallelly oriented shall be obtained. In Section 6, we shall present some useful theorems for the functional integrals over three-balls containing Wilson lines which meet the boundary at four points, two incoming and two outgoing. Next in Section 7, we shall develop the method further and obtain building blocks for the calculation of the link invariants. These are used to calculate the invariants for the knots upto seven crossing points as illustrations of the method in Section 8. Then we conclude with some remarks about generalizations of our results in Section 9. Appendix A contains some useful formulae for the $SU(2)$ quantum Racah coefficients and the duality matrix which relates the four point correlators of the $SU(2)_k$ Wess-Zumino conformal field theory. The field theoretic method developed here can be used to rederive many nice properties of the Jones polynomials ($n = 1$). As an illustration of these, we shall present a proof of the generalization of numerator-denominator theorem of Conway for Jones polynomials in Appendix B. In Appendix C we list some functional integrals over three manifolds containing Wilson lines ending on one or two boundaries, each an S^2 with four punctures, obtained by the method developed earlier. These functional integrals are used to obtain the knot invariants presented explicitly in Section 8.

2. Wilson Link-Operators in SU(2) Chern-Simons Theory in 3D

The metric independent action of Chern-Simons theory in a three-manifold M^3 is given by

$$kS = \frac{k}{4\pi} \int_{M^3} \text{tr}(AdA + \frac{2}{3}A^3) \quad (2.1)$$

where A is a matrix valued connection one-form of the gauge group G . In most of what follows we shall take the three manifold to be a three-sphere, S^3 . The topological operators of this topological field theory are given in terms of the Wilson loop (knot) operators:

$$W_R[C] = \text{tr}_R \text{Pexp} \oint_C A \quad (2.2)$$

for an oriented knot C . These operators depend both on the isotopy type of the knot as well as the representation R living on the knot through the matrix valued one-form $A_\mu = A_\mu^a T_R^a$ where T_R^a are the representation matrices corresponding to the representation R of the gauge group.

For a link $L = (C_1, C_2, \dots, C_s)$ made up of component knots C_1, C_2, \dots, C_s carrying representations R_1, R_2, \dots, R_s respectively, the Wilson link operator is defined as

$$W_{R_1 R_2 \dots R_s} [L] = \prod_{i=1}^s W_{R_i} [C_i] \quad (2.3)$$

Unless indicated explicitly otherwise, in the following we shall place the same representation R on all the component knots of a link and hence write the link operator $W_{R R \dots R} [L]$ simply as $W_R [L]$. The functional average of this link operator are the topological invariants of this theory. These we define as follows :

$$V_R [L] = \langle W_R [L] \rangle \equiv \frac{\int_{M^3} [dA] \prod_{i=1}^s W_R [C_i] e^{ikS}}{\int_{S^3} [dA] e^{ikS}} \quad (2.4)$$

Clearly these invariants depend only on the isotopy type of the oriented link L and the representation R placed on the component knots of the link. This is so because both the

integrand in the functional integral as well as the measure¹⁵ are independent of the metric of three-manifold on which the theory is defined.

These functional integrals can be evaluated by exploiting the connection of Chern-Simons theory on a three dimensional manifold with boundary to corresponding Wess-Zumino conformal field theory on the boundary⁴. Consider a three manifold M^3 with a set of two-dimensional boundaries $\Sigma^{(1)}, \Sigma^{(2)} \dots \Sigma^{(r)}$. Each of these boundaries $\Sigma^{(i)}$ may have a certain number of Wilson lines carrying representations $R_j^{(i)} (j = 1, 2 \dots)$ ending or beginning (at the punctures $P_j^{(i)}$) with representation $R_j^{(i)} (j = 1, 2 \dots)$ on them. With such a manifold we associate a state in the tensor product of Hilbert spaces $\otimes^r \mathcal{H}^{(i)}$ associated with these boundaries, each with a certain number of punctures. This state then will represent the functional integral of the Chern-Simons theory over such a manifold. The dimensionality of each of these Hilbert spaces $\mathcal{H}^{(i)}$ is given by the number of conformal blocks of the corresponding Wess-Zumino conformal field theory on the respective two dimensional boundaries with punctures $P_j^{(i)}$, $j = 1, 2 \dots$, carrying the primary fields in representations $R_j^{(i)}$, $j = 1, 2 \dots$, at these punctures.

Exploiting this connection with the Wess-Zumino conformal field theories, Witten has proved the following two very simple theorems for the link invariants (2.4).

Theorem 1: For the union of two distant (disjoint) oriented links (i.e., with no mutual entanglements) L_1, L_2 carrying representations R_1 and R_2

$$V_{R_1 R_2}[L] = V_{R_1}[L_1] V_{R_2}[L_2] \quad (2.5)$$

where $L = L_1 \sqcup L_2$.

Theorem 2: Given two oriented links L_1 and L_2 (Fig.1a) their connected sum $L_1 \# L_2$, is obtained as shown in Fig.1b. The strands that are joined have to have the same

representation living on them and also the orientations on them should match. Then the invariant for the connected sum is related to the invariant for the individual links as

$$V_R[L_1 \# L_2] = \frac{V_R[L_1]V_R[L_2]}{V_R[\cup]} \quad (2.6)$$


where $V_R[\cup]$ is the invariant of an unknot \cup (i.e., \bigcirc).

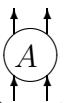
Besides these two theorems, within this field theoretic framework Witten has also proved the Alexander-Conway skein relation for the case where the fundamental representation lives on all the components of the link. We shall now present a derivation of the generalized Alexander-Conway skein relations for arbitrary representations living on the links.

3. Recursion Relations Among the Link Invariants

Before deriving recursion relations among the link invariants, let us introduce a few useful definitions.

Following, Lickorish and Millet¹⁶, we shall call a compact 3-dimensional submanifold in S^3 with the boundary carrying a finite set of points marked by arrows as “in” or “out”, a room. An inhabitant of the room is a properly embedded smooth, compact oriented 1-manifold which meets the boundary of the room at the given set of points with its orientation matching with the “in” and “out” designations. Examples of rooms are shown in Fig.2. Here 2(a) is a three-ball with no markings on its boundary; 2(b) is a three-ball with two marked points on its boundary, one “in” and one “out”; 2(c) is a three-ball with four marked points on the boundary, two “in” and two “out”. Fig.2(d) shows a room with two inlets and two outlets with an example of an inhabitant of the room drawn explicitly.

Now let us consider a link $L_m(A)$ as shown in Fig.3(a) made up of a room  with its parallelly oriented lower two strands containing a certain number of half-twists m and then joined to the upper two strands of the room as shown. The half-twists are taken to be positive or negative if these are right-handed or left-handed respectively as shown in Fig.4. Thus m can be $0, \pm 1, \pm 2, \pm 3, \dots$ in the link $L_m(A)$ of Fig.3(a). On each component of this link, we place the spin $n/2$ representation R_n of $SU(2)$ given by Young tableaux with n horizontal boxes.

Following Witten⁴, we cut out a ball B_1 containing the room  as well as all the twists in the lower two strands of this room as shown in Fig.5(b). The boundary S^2 of this ball is punctured at two “in” and two “out” points. The normalized functional integral over this ball will be represented by $\psi_m(A)$. The rest of S^3 containing the remaining part of the link $L_m(A)$ is also a three-ball (B_2) with an oppositely oriented S^2 with four punctures (two “in” and two “out”) as its boundary as shown in Fig.5(b). The normalized functional integral over this ball is represented by $\bar{\psi}_0$. These two normalized functional integrals, $\psi_m(A)$ and $\bar{\psi}_0$ are vectors in two mutually dual Hilbert spaces, \mathcal{H} and $\bar{\mathcal{H}}$, associated with the two oppositely oriented S^2 's forming the boundaries of the two balls B_1 and B_2 respectively. Each of this S^2 has four punctures with representations R_n attached to them. The dimensionality of each of these two vector spaces is given by the number of conformal blocks of the correlator for four primary fields, each in representation R_n , of the corresponding Wess-Zumino $SU(2)_k$ conformal field theory on S^2 . The fusion rules of this conformal field theory are given by: $R_n \otimes R_n = \bigoplus_{j=0}^n R_{2j}$, for $k \geq 2n$. (For $k < 2n$ the representations with $2j > k$ on the right hand side are not integrable and hence are not to be included in the fusion rules). We shall restrict our discussion to the case $k \geq 2n$. However, the method developed here can also be used for $k < 2n$. The number of conformal blocks for the above four-point correlator is the number of singlets in the decomposition of $R_n \otimes R_n \otimes R_n \otimes R_n$, which by the fusion rules is simply $n + 1$.

Hence the dimensionality of each of the vector spaces \mathcal{H} and $\overline{\mathcal{H}}$ is $(n + 1)$ and normalized functional integrals $|\psi_m(A)\rangle$ and $|\overline{\psi}_0\rangle$ are $(n + 1)$ dimensional vectors in these spaces, respectively.

Now glueing back the balls B_1 and B_2 gives us the original link $L_m(A)$. Thus the invariant $V_n[L_m(A)]$ for this link can be represented through the natural contraction of the vectors $|\psi_m(A)\rangle$ and $|\overline{\psi}_0\rangle$ in the mutually dual Hilbert spaces, \mathcal{H} and $\overline{\mathcal{H}}$, respectively:

$$V_n[L_m(A)] = \langle \overline{\psi}_0 | \psi_m(A) \rangle \quad (3.1)$$

Here the subscript n indicates that the representation R_n with its Young tableaux containing n boxes is living on all the component knots.

Now the vector $|\psi_m(A)\rangle$ represents normalized functional integral over the ball B_1 with m half-twists in the inner two strands as shown in the Fig.3(b). The operation of introducing a half-twist in these two strands can be represented by an $(n + 1) \times (n + 1)$ matrix, \tilde{B} operating on these vectors $|\psi_m(A)\rangle$ in the $(n + 1)$ dimensional Hilbert space \mathcal{H} . Thus we may write

$$(\tilde{B})^j |\psi_l(A)\rangle = |\psi_{l+j}(A)\rangle, \quad j = \pm 1, \pm 2, \dots$$

The characteristic equation of the $(n + 1) \times (n + 1)$ half-twist monodromy matrix \tilde{B} can be written as

$$\sum_{j=\ell}^{n+\ell+1} \tilde{\alpha}_{j-\ell} (\tilde{B})^j = 0, \quad \ell = 0, \pm 1, \pm 2, \dots \quad (3.2)$$

where the coefficients $\tilde{\alpha}_0, \tilde{\alpha}_1, \dots, \tilde{\alpha}_{n+1}$ in terms of the eigen-values $\tilde{\lambda}_i, i = 0, 1, \dots, n$, of the matrix \tilde{B} are

$$\begin{aligned} \tilde{\alpha}_0 &= (-1)^{n+1} \prod_{i=0}^n \tilde{\lambda}_i, \\ \tilde{\alpha}_1 &= (-1)^n \sum_{\substack{0 \\ i_1 \neq i_2 \neq \dots \neq i_n}}^n \tilde{\lambda}_{i_1} \tilde{\lambda}_{i_2} \dots \tilde{\lambda}_{i_n}, \end{aligned}$$

$$\begin{aligned}
& \vdots \\
\tilde{\alpha}_{n-1} &= (-1)^2 \sum_{\substack{0 \\ i_1 \neq i_2}}^n \tilde{\lambda}_{i_1} \tilde{\lambda}_{i_2}, \\
\tilde{\alpha}_n &= \sum_0^n \tilde{\lambda}_i, \\
\tilde{\alpha}_{n+1} &= 1
\end{aligned} \tag{3.3}$$

The eigen-values of the matrix \tilde{B} are given by the monodromy properties of the four-point correlator for the primary fields, all in representation R_n , of $SU(2)_k$ Wess-Zumino conformal field theory on S^2 (ref. 17):

$$\tilde{\lambda}_j = (-1)^{n-j} \exp[i\pi(2h_n - h_{2j})], \quad j = 0, 1, \dots, n \tag{3.4}$$

where $h_j = \frac{j}{2}(\frac{j}{2} + 1)/(k + 2)$ is the conformal weight of the primary field of spin $j/2$ representation R_j of the $SU(2)_k$ Wess-Zumino conformal field theory.

Applying Eqn.(3.2) on the vector $|\psi_o(A)\rangle$ with no twists, yields an equation amongst these vectors with successively increasing number of half-twists as :

$$\sum_{j=\ell}^{n+\ell+1} \tilde{\alpha}_{j-\ell} |\psi_j(A)\rangle = 0, \quad \ell = 0, \pm 1, \pm 2, \dots \tag{3.5}$$

which in turn, using (3.1), yields a relation amongst link invariants $L_m(A)$ as

$$\sum_{j=\ell}^{\ell+n+1} \tilde{\alpha}_{j-\ell} V_n[L_j(A)] = 0, \quad \ell = 0, \pm 1, \pm 2, \dots \tag{3.6}$$

The link invariants may be given with respect to some reference framing. Generally these are given in standard framing wherein each component knot of the link has its self-linking number as zero. Notice that the half-twist matrix \tilde{B} above does not preserve the framing. Thus the various link invariants in Eqn.(3.6) are not in the same framing. In order to have all the links in standard framing, the coefficients, $\tilde{\alpha}_m, m = 0, 1 \dots n + 1$ in (3.6) need to be multiplied by $\exp(-2i\pi m h_n)$, respectively to cancel the change in framing

due to twisting. We implement this change in Eqns.(3.2)-(3.6) and for convenience divide all of them by an over all factor $\exp(-2i\pi(n+1)h_n)$. This makes the effective half-twist monodromy matrix for parallelly oriented strands to be $B = \exp(2i\pi h_n)\tilde{B}$. Its eigenvalues are given by :

$$\lambda_j = (-)^{n-j} q^{\frac{(n(n+2)-j(j+1))}{2}} \quad j = 0, 1, \dots, n \quad (3.7)$$

with $q = \exp[2i\pi/(k+2)]$, instead of those in Eqn.(3.4). Thus we rewrite the final generalized Alexander-Conway skein recursion relation in the form of the following theorem:

Theorem 3: The link invariants for links $L_m(A)$ of Fig.3 are related as:

$$\sum_{j=\ell}^{\ell+n+1} \alpha_{j-\ell} V_n[L_j(A)] = 0, \quad \ell = 0, \pm 1, \pm 2 \dots \quad (3.8)$$

where the coefficients α_i are given in terms of the eigenvalues of the effective half-twist matrix B above (Eqn.3.7) as :

$$\begin{aligned} \alpha_0 &= (-1)^{n+1} \prod_{i=0}^n \lambda_i, \\ \alpha_1 &= (-1)^n \sum_{\substack{0 \\ i_1 \neq i_2 \neq \dots \neq i_n}}^n \lambda_{i_1} \lambda_{i_2} \dots \lambda_{i_n}, \\ &\vdots \\ \alpha_{n-1} &= (-1)^2 \sum_{\substack{0 \\ i_1 \neq i_2}}^n \lambda_{i_1} \lambda_{i_2}, \\ \alpha_n &= \sum_0^n \lambda_i, \\ \alpha_{n+1} &= 1 \end{aligned} \quad (3.9)$$

This recursion relation has also been obtained in ref.14 within the field theoretic formulation. An earlier derivation of this recursion relation within the frame-work of exactly solvable models is presented in ref.10.

Now let us list some special cases of this relation : **(i)n=1:** Here the two eigen values of the effective monodromy matrix B are $\lambda_o = -q^{3/2}$ and $\lambda_1 = q^{1/2}$, so that $\alpha_o = -q^2$, $\alpha_1 = q^{3/2} - q^{1/2}$ and $\alpha_2 = 1$. These lead to the three-element recursion relation for the Jones polynomials as

$$-qV_1[L_\ell(A)] + (q^{1/2} - q^{-1/2})V_1[L_{\ell+1}(A)] + q^{-1}V_1[L_{\ell+2}(A)] = 0, \quad \ell = 0, \pm 1, \pm 2 \dots \quad (3.10)$$

(ii)n=2: Here $\lambda_o = q^4$, $\lambda_1 = -q^3$, $\lambda_2 = q$, and therefore, $\alpha_o = q^8$, $\alpha_1 = -q^7 + q^5 - q^4$, $\alpha_2 = -q^4 + q^3 - q$ and $\alpha_3 = 1$. This leads to the four-element recursion relation:

$$q^4V_2[L_\ell(A)] - (q^3 - q + 1)V_2[L_{\ell+1}(A)] - (q^{-3} - q^{-1} + 1)V_2[L_{\ell+2}(A)] + q^{-4}V_2[L_{\ell+3}(A)] = 0, \quad \ell = 0, \pm 1, \pm 2 \dots \quad (3.11)$$

(iii)n=3: Here $\lambda_o = -q^{15/2}$, $\lambda_1 = q^{13/2}$, $\lambda_2 = -q^{9/2}$, $\lambda_3 = q^{3/2}$, and hence, $\alpha_o = q^{20}$, $\alpha_1 = -q^{37/2} - q^{27/2} + q^{31/2} + q^{25/2}$, $\alpha_2 = -q^{14} + q^{12} - q^{11} - q^9 + q^8 - q^6$, $\alpha_3 = q^{15/2} - q^{13/2} + q^{9/2} - q^{3/2}$, $\alpha_4 = 1$. The recursion relation here has five elements:

$$q^{10}V_3[L_\ell] - (q^{17/2} - q^{11/2} + q^{7/2} - q^{5/2})V_3[L_{\ell+1}] - (q^4 - q^2 + q + q^{-1} - q^{-2} + q^{-4})V_3[L_{\ell+2}] - (q^{-17/2} - q^{-11/2} + q^{-7/2} - q^{-5/2})V_3[L_{\ell+3}] + q^{-10}V_3[L_{\ell+4}] = 0, \quad \ell = 0, \pm 1, \pm 2 \dots \quad (3.12)$$

Now we shall present two more recursion relations which can be obtained on the same lines as above.

4. New Recursion Relations

Let us consider a link $\hat{L}_{2m}(\hat{A})$ as shown in Fig.5a, which has even number of half-twists $2m$, in the oppositely oriented inner two strands. This link can be obtained by glueing two balls B_1 and B_2 as shown in Fig.5b, along their oppositely oriented boundaries. The normalized functional integrals over these two balls are represented by two $(n+1)$

dimensional vectors $|\chi_{2m}(\hat{A})\rangle$ and $|\bar{\chi}_o\rangle$ in the two $(n+1)$ dimensional mutually dual Hilbert spaces associated with the two four-punctured S^2 's forming the boundaries of these two balls respectively. The invariant for this link is given by the natural contraction of these two vectors :

$$V_n[\hat{L}_{2m}(\hat{A})] = \langle \bar{\chi}_o | \chi_{2m}(\hat{A}) \rangle \quad (4.1)$$

Let \hat{B} be the $(n+1) \times (n+1)$ matrix introducing half-twists in oppositely oriented inner two strands in the ball B_1 . Then

$$(\hat{B}^2)^j |\chi_{2m}(\hat{A})\rangle = |\chi_{2m+2j}(\hat{A})\rangle, \quad j = \pm 1, \pm 2, \dots \quad (4.2)$$

The eigen-values of this matrix \hat{B} introducing half-twists in oppositely oriented strands on a four-punctured S^2 , are given by

$$\hat{\lambda}_\ell = (-)^{\ell} q^{\ell(\ell+1)/2} \quad \ell = 0, 1, \dots, n \quad (4.3)$$

The characteristic equation for \hat{B}^2 yields:

$$\sum_{j=\ell}^{\ell+n+1} \hat{\alpha}_{j-\ell} \hat{B}^{2j} = 0 \quad (4.4)$$

and therefore

$$\sum_{j=\ell}^{n+\ell+1} \hat{\alpha}_{j-\ell} |\chi_{2j}(\hat{A})\rangle = 0 \quad (4.5)$$

where $\hat{\alpha}_i, i = 0, 1, \dots, n+1$ are related to the eigen values of the \hat{B}^2 matrix in the usual way given below in Eqn.(4.7). Thus this yields us a recursion relation for the link invariants:

Theorem 4: The invariants for the links in Fig.5a are related as

$$\sum_{j=\ell}^{n+\ell+1} \hat{\alpha}_{j-\ell} V_n[\hat{L}_{2j}(\hat{A})] = 0, \quad \ell = 0, \pm 1, \pm 2 \dots \quad (4.6)$$

where the coefficients $\hat{\alpha}_i$ are given by

$$\hat{\alpha}_0 = (-1)^{n+1} \prod_{i=0}^n \hat{\lambda}_i^2,$$

$$\begin{aligned}
\hat{\alpha}_1 &= (-1)^n \sum_{\substack{0 \\ i_1 \neq i_2 \neq \dots \neq i_n}}^n \hat{\lambda}_{i_1}^2 \hat{\lambda}_{i_2}^2 \dots \hat{\lambda}_{i_n}^2, \\
&\vdots \\
\hat{\alpha}_{n-1} &= (-1)^2 \sum_{\substack{0 \\ i_1 \neq i_2}}^n \hat{\lambda}_{i_1}^2 \hat{\lambda}_{i_2}^2, \\
\hat{\alpha}_n &= \sum_0^n \hat{\lambda}_i^2, \\
\hat{\alpha}_{n+1} &= 1
\end{aligned} \tag{4.7}$$

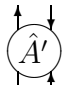
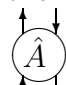
Here $\hat{\lambda}_i$ are the eigenvalues of \hat{B} matrix given in Eq.(4.3).

Now let us present a few special cases of this theorem: **(i)n=1:** Here the two eigenvalues of the monodromy matrix \hat{B} are $\hat{\lambda}_0 = 1$, $\hat{\lambda}_1 = -q$. Thus $\hat{\alpha}_0 = q^2$, $\hat{\alpha}_1 = -(1 + q^2)$, $\hat{\alpha}_2 = 1$. The recursion relations for $\ell = 0, \pm 1, \pm 2 \dots$, then read :

$$qV_1[\hat{L}_{2\ell}(\hat{A})] - (q + q^{-1})V_1[\hat{L}_{2\ell+2}(\hat{A})] + q^{-1}V_1[\hat{L}_{2\ell+4}(\hat{A})] = 0 \tag{4.8}$$

(ii)n=2: Here the eigenvalues of \hat{B} are $\hat{\lambda}_0 = 1$, $\hat{\lambda}_1 = -q$, $\hat{\lambda}_2 = q^3$ so that $\hat{\alpha}_0 = -q^8$, $\hat{\alpha}_1 = q^2 + q^6 + q^8$, $\hat{\alpha}_2 = -(1 + q^2 + q^6)$ and $\hat{\alpha}_3 = 1$. The recursion relations for $\ell = 0, \pm 1 \pm 2 \dots$, then read :

$$\begin{aligned}
&-q^4V_2[\hat{L}_{2\ell}(\hat{A})] + (q^{-2} + q^2 + q^4)V_2[\hat{L}_{2\ell+2}(\hat{A})] - \\
&\quad (q^{-4} + q^{-2} + q^2)V_2[\hat{L}_{2\ell+4}(\hat{A})] + q^{-4}V_2[\hat{L}_{2\ell+6}(\hat{A})] = 0
\end{aligned} \tag{4.9}$$

Similar recursion relations can be obtained for links shown in Fig.6 which have odd number of half-twists in the oppositely oriented middle two strands with the room  as indicated in the Fig.6. This room is to be contrasted with the room  in Fig.5a. An analysis as above then leads to the theorem:



Theorem 5: For links $\hat{L}_{2m+1}(\hat{A}')$ as shown in Fig.6, the link invariants are related as

$$\sum_{j=\ell}^{n+\ell+1} \hat{\alpha}_{j-\ell} V_n[\hat{L}_{2j+1}(\hat{A}')] = 0 \quad (4.10)$$

where $\hat{\alpha}_i$, $i = 0, 1, \dots, n+1$ are given by equations (4.7) above.

The recursion relation given in Theorems 3 - 5 do relate various link invariants. However, it is only for $n = 1$ (Jones Polynomials) that the Alexander-Conway skein relation (3.10) along with the factorization property of disjoint links given by Theorem 1 is complete. That is, this can recursively be solved for the link invariant of an arbitrary link. For $n = 2$ and higher, this is not so. Additional information is required to obtain the link invariants. Alternatively, methods need to be developed to obtain the link invariants directly. In the following sections, we shall present one such method within the field theoretic frame work.

5. Invariants for Links Obtained as Closures of Two Strand Braids

Consider the link $L_m(A_1, A_2)$ obtained by glueing two balls along their oppositely oriented boundaries S^2 's as shown in Fig.7. The ball B_1 contains the room  with the lower two strands oriented in the same direction and containing m half-twists. The ball B_2 contains the room . The two boundaries are two S^2 's with four punctures each, two "in" and two "out". The normalized functional integrals over these two balls are represented by vectors $|\psi_m(A_1)\rangle$ and $|\bar{\psi}_0(A_2)\rangle$ in two mutually dual $(n+1)$ dimensional vector spaces \mathcal{H} and $\bar{\mathcal{H}}$ respectively. Let $|\phi_\ell\rangle$, $\ell = 0, 1, \dots, n$ be a complete orthonormal set of eigen-vectors in \mathcal{H} of the braid matrix B which introduces half-twists in the inner two parallel strands in B_1 in Fig. 7a :

$$B |\phi_\ell\rangle = \lambda_\ell |\phi_\ell\rangle,$$

$$\lambda_\ell = (-)^{n-\ell} q^{\frac{n(n+2)-\ell(\ell+1)}{2}}, \quad \ell = 0, 1, 2, \dots, n \quad (5.1)$$

The corresponding vectors in dual Hilbert space are denoted by $|\phi^\ell\rangle$ and the pairing of these is given by $\langle\phi^\ell | \phi_j\rangle = \delta_j^\ell$. The vectors $|\psi_0(A_1)\rangle$ and $|\bar{\psi}_0(A_2)\rangle$ can then be expanded in terms of these bases :

$$\begin{aligned} |\psi_0(A_1)\rangle &= \sum_{\ell=0}^n \mu_\ell(A_1) |\phi_\ell\rangle \\ \langle\bar{\psi}_0(A_2) | &= \sum_{\ell=0}^n \mu_\ell(A_2) \langle\phi^\ell | \end{aligned} \quad (5.2)$$

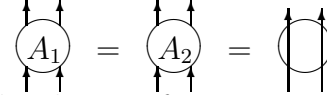
The vector with m half-twists ($m = 0, \pm 1, \pm 2, \dots$) is

$$|\psi_m(A_1)\rangle = \sum_{\ell=0}^n \mu_\ell(A_1) (\lambda_\ell)^m |\phi_\ell\rangle \quad (5.3)$$

The invariant for the link $L_m(A_1, A_2)$ of Fig.7, then can be written as the contraction of the vector $|\psi_m(A_1)\rangle$ and $|\bar{\psi}_0(A_2)\rangle$ as :

$$V_n[L_m(A_1, A_2)] = \sum_{\ell=0}^n \mu_\ell(A_1) \mu_\ell(A_2) (\lambda_\ell)^m \quad (5.4)$$

Now if we can obtain a systematic method of finding the coefficients

$\mu_\ell(A_1)$ and $\mu_\ell(A_2)$, we can write down these link invariants. To do so let us take the two rooms to be . Then the link $L_m(A_1, A_2)$ is simply the link \mathcal{L}_m obtained as the closure of m times twisted braid of two parallelly oriented strands as shown in Fig.8. Writing simply μ_ℓ for $\mu_\ell(\text{circle with four arrows})$, the invariant for this link is

$$V_n[\mathcal{L}_m] = \sum_{\ell=0}^n \mu_\ell \mu_\ell (\lambda_\ell)^m \quad (5.5)$$

Now we need to determine μ_ℓ . Notice \mathcal{L}_0 is simply two unknots unlinked $\cup \sqcup \cup$; $\mathcal{L}_{\pm 1}$ are both one unknot \cup ; $\mathcal{L}_{\pm 2}$ are right/left handed Hopf links (H, H^*) and $\mathcal{L}_{\pm 3}$ are right/left handed trefoil knots (T, T^*) . Thus we may write

$$\begin{aligned} V_n[\mathcal{L}_0] &= (V_n[\cup])^2 = \sum_{\ell=0}^n \mu_\ell \mu_\ell \\ V_n[\mathcal{L}_{\pm 1}] &= V_n[\cup] = \sum_{\ell=0}^n \mu_\ell \mu_\ell (-)^{n-\ell} q^{\pm \frac{n(n+2)}{2} \mp \frac{\ell(\ell+1)}{2}} \end{aligned} \quad (5.6)$$

where we have used Theorem 1 to write $V_n[\cup \sqcup \cup] = (V_n[\cup])^2$. From the second relation above, it is clear that $V_n[\cup]$ is invariant under $q \rightarrow q^{-1}$. This is so because unknot has no chirality. These two equations can be solved recursively for various values of n . For $n = 0$, we have $\mu_0 = 1$. Then using this, for $n = 1$, we obtain from these relations $\mu_1 = \sqrt{[3]}$. For $n = 2$, next we obtain $\mu_2 = \sqrt{[5]}$. Thus in general $\mu_\ell = \sqrt{[2\ell + 1]}$, where $[m]$ is the q -number defined as

$$[m] = \frac{q^{m/2} - q^{-m/2}}{q^{1/2} - q^{-1/2}} \quad (5.7)$$

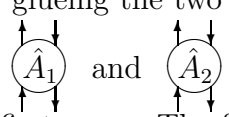
Using these in the first equation in (5.6) and the identity $\sum_{\ell=0}^n [2\ell + 1] = [n + 1]^2$ we have the knot invariant for the unknot as

$$V_n[\cup] = [n + 1] \quad (5.8)$$

This is not surprising, because the link invariant for two cabled knots such as the two unlinked unknots obey the fusion rules. That is, as can be checked readily, the expression (5.8) for unknot obey the fusion rule $V_{n_1}[\cup]V_{n_2}[\cup] = \sum_{j=0}^{\min(n_1, n_2)} V_{|n_1 - n_2| + 2j}[\cup]$. We can now put all this together in the form of a theorem :

Theorem 6: For links \mathcal{L}_m obtained as the closure of a braid of two parallelly oriented strands with m half-twists (Fig.8) the link invariant is given by

$$V_n[\mathcal{L}_m] = \sum_{\ell=0}^n (-)^{m(n-\ell)} q^{\frac{m}{2}(n(n+2)-\ell(\ell+1))} [2\ell + 1], \quad m = 0, \pm 1, \pm 2 \dots \quad (5.9)$$

A similar discussion can be carried through for the links of the type shown in Fig.9 and Fig.10. The link $\hat{L}_{2m}(\hat{A}_1, \hat{A}_2)$ is obtained by glueing the two connected balls B_1 and B_2 as shown in Fig.9. Here we have two rooms  with $2m$ half-twists in the oppositely oriented lower two strands of the first room. The functional integrals over these two balls are again given by vectors $|\chi_{2m}(\hat{A}_1)\rangle$ and $|\bar{\chi}_0(A_2)\rangle$ in mutually dual $n + 1$

dimensional Hilbert spaces associated with oppositely oriented four-punctured S^2 . The invariant of this link is given by natural contraction of these two vectors. Here the braid matrix \hat{B} introduces half-twists now in oppositely oriented middle two strands of ball B_1 , $|\chi_{2m}(\hat{A}_1)\rangle = \hat{B}^{2m} |\chi_0(\hat{A}_1)\rangle$. Let $|\hat{\phi}_\ell\rangle$ be a complete set of eigenfunctions, in vector space \mathcal{H} , of this braid matrix \hat{B} ,

$$\hat{B} |\hat{\phi}_\ell\rangle = \hat{\lambda}_\ell |\hat{\phi}_\ell\rangle, \quad \hat{\lambda}_\ell = (-)^\ell q^{\frac{\ell(\ell+1)}{2}}, \quad \ell = 0, 1, \dots, n \quad (5.10)$$

The corresponding basis in the dual Hilbert space are denoted by $|\hat{\phi}^\ell\rangle$, with their natural contraction as $\langle \hat{\phi}^\ell | \hat{\phi}_j \rangle = \delta_j^\ell$. Expand $|\chi_0(\hat{A}_1)\rangle$ and $\langle \bar{\chi}_0(\hat{A}_2) |$ in these bases :

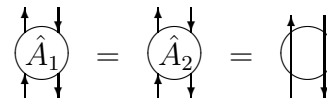
$$\begin{aligned} |\chi_0(\hat{A}_1)\rangle &= \sum_{\ell=0}^n \hat{\mu}_\ell(\hat{A}_1) |\hat{\phi}_\ell\rangle \\ \langle \bar{\chi}_0(\hat{A}_2) | &= \sum_{\ell=0}^n \hat{\mu}_\ell(\hat{A}_2) \langle \hat{\phi}^\ell | \end{aligned} \quad (5.11)$$

Then the vector with 2m half-twists is

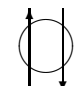
$$|\chi_{2m}(\hat{A}_1)\rangle = \sum \hat{\mu}_\ell(\hat{A}_1) (\hat{\lambda}_\ell)^{2m} |\hat{\phi}_\ell\rangle \quad (5.12)$$

so that the link invariant for the links of Fig.9 are given by

$$V_n[\hat{L}_{2m}(\hat{A}_1, \hat{A}_2)] = \sum_{\ell=0}^n \hat{\mu}_\ell(\hat{A}_1) \hat{\mu}_\ell(\hat{A}_2) (\hat{\lambda}_\ell)^{2m} \quad (5.13)$$

In particular, if we take the two rooms to be  , then the link $\hat{L}_{2m}(\hat{A}_1, \hat{A}_2)$ simply becomes the link $\hat{\mathcal{L}}_{2m}$ obtained as the closure of two oppositely oriented strands with 2m half-twists as shown in Fig.10. The invariants for these links can be written as

$$V_n[\hat{\mathcal{L}}_{2m}] = \sum_{\ell=0}^n \hat{\mu}_\ell \hat{\mu}_\ell (\hat{\lambda}_\ell)^{2m} \quad (5.14)$$

where $\hat{\mu}_\ell$ here refer to the room  . Now, since $\hat{\mathcal{L}}_0 = \cup \sqcup \cup$ and $\hat{\mathcal{L}}_{\pm 2}$ are right/left handed Hopf links (H, H^*) , using $V_n[\cup] = [n+1]$ and $V_n[H] = 1 + q + q^2 + \dots + q^{n(n+2)}$ and

$V_n[H^*] = 1 + q^{-1} + q^{-2} + \dots + q^{-n(n+2)}$ as obtained using Theorem 6, we can solve for these $\hat{\mu}_\ell$'s successively for $n = 0, 1, 2, \dots$. This yields

$$\hat{\mu}_\ell = \mu_\ell = \sqrt{[2\ell + 1]}.$$

Thus we collect these results into a theorem.

Theorem 7: For links $\hat{\mathcal{L}}_{2m}$ obtained as the closure of a braid made up of two oppositely oriented strands containing $2m$ half- twists (Fig.10) the invariants are :

$$V_n[\hat{\mathcal{L}}_{2m}] = \sum_{\ell=0}^n [2\ell + 1] q^{m\ell(\ell+1)}, \quad m = 0, \pm 1, \pm 2, \dots \quad (5.15)$$

After presenting these two simple theorems, we wish to develop this method further to obtain link invariants for more complicated links. This we do in the next section.

6. Some Useful Theorems for Link Invariants

Consider the two rooms Q_m^V and Q_{2p+1}^H with four markings as indicated in Fig 11a. The first one has m half-twists vertically in the parallelly oriented strands and the latter has $2p + 1$ half-twists horizontally in the oppositely oriented strands. The functional integral over the ball containing these rooms (Fig 11b) may be represented by vectors $|\psi(Q_m^V)\rangle$ and $|\psi(Q_{2p+1}^H)\rangle$ respectively. The vector $|\psi(Q_m^V)\rangle$ is obtained by applying the braid matrix B (with eigenvalues $\lambda_\ell = (-)^{n-\ell} q^{\frac{n(n+2)}{2} - \frac{\ell(\ell+1)}{2}}$ and eigenfunctions denoted by $|\phi_\ell\rangle, \ell = 0, 1, \dots, n$) of the parallelly oriented central two strands m times on the vector $|\psi(Q_o^V)\rangle$. This vector from the discussion of the previous section can be represented in terms of the normalised eigenfunctions of B as

$$|\psi(Q_o^V)\rangle = \sum_{\ell=0}^n \sqrt{[2\ell + 1]} |\phi_\ell\rangle \quad (6.1)$$

On the other hand, the vector $|\psi(Q_{2p+1}^H)\rangle$ can be thought of as obtained by applying the braiding matrix \hat{B} (with eigenvalues $\hat{\lambda}_\ell = (-)^{\ell} q^{\frac{\ell(\ell+1)}{2}}$ and eigenfunctions denoted by $|\hat{\phi}_\ell\rangle$, $\ell = 0, 1, 2, \dots, n$) of anti-parallelly oriented side two strands in Fig11b on the vector

$$|\psi(Q_0^H)\rangle = \sum_{\ell=0}^n \sqrt{[2\ell + 1]} |\hat{\phi}_\ell\rangle \quad (6.2)$$

which has been expanded in terms of the eigenfunctions $|\hat{\phi}_\ell\rangle$ following the discussion of the previous section. The basis referring to the first two strands on the left (or equivalently the last two on the right) in Fig.11b, $|\hat{\phi}_\ell\rangle$ and those referring to the inner two strands $|\phi_\ell\rangle$ are connected by the matrix $a_{j\ell} = \langle\phi^\ell | \hat{\phi}_j\rangle$ where $\langle\phi^\ell |$ refers to the basis with respect to the central two strands in the dual Hilbert space obtained by changing the orientation of the boundary S^2 of the ball. This discussion immediately allows us to write down the following theorem.

Theorem 8: The functional integrals $|\psi(Q_m^V)\rangle$ and $|\psi(Q_{2p+1}^H)\rangle$ for the balls as shown in Fig 11b can be written in terms of the basis $|\phi_\ell\rangle$ referring to the parallelly oriented middle two strands as :

$$\begin{aligned} |\psi(Q_m^V)\rangle &= \sum_{\ell=0}^n \mu_\ell(Q_m^V) |\phi_\ell\rangle \\ |\psi(Q_{2p+1}^H)\rangle &= \sum \mu_\ell(Q_{2p+1}^H) |\phi_\ell\rangle \end{aligned}$$

with

$$\begin{aligned} \mu_\ell(Q_m^V) &= (-1)^{m(n-\ell)} q^{\frac{m}{2}(n(n+2)-\ell(\ell+1))} \sqrt{[2\ell + 1]} \\ \mu_\ell(Q_{2p+1}^H) &= \sum_{j=0}^n (-1)^j q^{(2p+1)\frac{j(j+1)}{2}} \sqrt{[2j + 1]} a_{j\ell} \end{aligned} \quad (6.3)$$

Here $\mu_\ell(Q_{2p+1}^H)$ is obtained by first expanding in terms of the basis $|\hat{\phi}_\ell\rangle$ referring to the first two strands and then changing the basis to $|\phi_\ell\rangle$ which refers to the middle two strands, $|\hat{\phi}_j\rangle = \sum_{\ell=0}^n a_{j\ell} |\phi_\ell\rangle$.

Similar discussion can be gone through with regard to the rooms \hat{Q}_m^V , \hat{Q}_{2p}^H and $\hat{Q}_p^{H'}$ as shown in Fig 12a and the corresponding functional integrals for these balls (redrawn in Fig 12b), $|\chi(\hat{Q}_m^V)\rangle$, $|\chi(\hat{Q}_{2p}^H)\rangle$ and $|\chi(\hat{Q}_p^{H'})\rangle$ respectively. The middle two strands here (Fig 12b) in all cases are oppositely oriented. The basis $|\hat{\phi}_\ell\rangle$ referring to these are eigen functions of braid matrix \hat{B} with eigenvalues $(-)^{\ell}q^{\ell(\ell+1)/2}$, $\ell = 0, 1, \dots, n$. For the vector $|\chi(\hat{Q}_{2p}^H)\rangle$, the braid matrix with respect to the first two strands which are also oppositely oriented has the same eigenvalues. On the other hand the braid matrix with respect to the first two strands in $|\chi(\hat{Q}_p^{H'})\rangle$ which are parallelly oriented, has the eigenvalues $(-)^{n-\ell}q^{\frac{n(n+2)}{2}-\frac{\ell(\ell+1)}{2}}$, $\ell = 0, 1, \dots, n$. This discussion, therefore, immediately leads to the theorem:

Theorem.9: The functional integrals $|\chi(\hat{Q}_m^V)\rangle$, $|\chi(\hat{Q}_{2p}^H)\rangle$ and $|\chi(\hat{Q}_p^{H'})\rangle$ for the balls as shown in Fig 12b can be written in terms of the basis $|\hat{\phi}_\ell\rangle$ referring to the anti-parallelly oriented middle two strands as

$$\begin{aligned} |\chi(\hat{Q}_m^V)\rangle &= \sum_{\ell=0}^n \hat{\mu}_\ell(\hat{Q}_m^V) |\hat{\phi}_\ell\rangle \\ |\chi(\hat{Q}_{2p}^H)\rangle &= \sum \hat{\mu}_\ell(\hat{Q}_{2p}^H) |\hat{\phi}_\ell\rangle \\ |\chi(\hat{Q}_p^{H'})\rangle &= \sum \mu_\ell(\hat{Q}_p^{H'}) |\hat{\phi}_\ell\rangle \end{aligned}$$

where

$$\begin{aligned} \hat{\mu}_\ell(\hat{Q}_m^V) &= (-)^{m\ell} q^{\frac{m\ell(\ell+1)}{2}} \sqrt{[2\ell+1]} \\ \hat{\mu}_\ell(\hat{Q}_{2p}^H) &= \sum_{j=0}^n q^{pj(j+1)} \sqrt{[2j+1]} a_{j\ell} \\ \hat{\mu}_\ell(\hat{Q}_p^{H'}) &= \sum_{j=0}^n (-)^{p(n-j)} q^{p(\frac{n(n+2)}{2}-\frac{j(j+1)}{2})} \sqrt{[2j+1]} a_{j\ell} \end{aligned} \quad (6.4)$$

Here again the matrix $a_{j\ell}$ relates basis with respect to the first two strands (or equivalently last two strands) with the basis with respect to the middle two strands in Fig 12b.

The matrix $a_{j\ell}$ has very interesting properties. To see this, let us glue two balls containing the rooms \hat{Q}_{2m}^H and \hat{Q}_{2p}^H respectively to obtain the link $\hat{L}_0(\hat{Q}_{2m}^H, \hat{Q}_{2p}^H)$ as shown in Fig 13a. This link is the same as link $\hat{\mathcal{L}}_{2m+2p}$ obtained by the closure of the braid of two anti-parallel strands with $2m+2p$ half-twists discussed in the previous section. Then the invariant for this link $V_n[\hat{L}_o(\hat{Q}_{2m}^H, \hat{Q}_{2p}^H)]$ can be written as

$$\sum_{\ell=0}^n \hat{\mu}_\ell(\hat{Q}_{2m}^H) \hat{\mu}_\ell(\hat{Q}_{2p}^H) = \sum_{\ell=0}^n q^{(m+p)\ell(\ell+1)} \sqrt{[2\ell+1]}$$

In this we substitute $\hat{\mu}_\ell(\hat{Q}_{2m}^H)$ and $\hat{\mu}_\ell(\hat{Q}_{2p}^H)$ from Eqn 6.4. Since this equation is valid for arbitrary m and p , we can equate the coefficients of various powers of q^m , q^p . This immediately yields :

$$\sum_{\ell=0}^n a_{i\ell} a_{j\ell} = \delta_{ij} \quad (6.5)$$

On the other hand, if we compose two balls containing the rooms \hat{Q}_{2m}^H and \hat{Q}_{2p}^V as shown in Fig 13b, we have the links $\hat{L}_o(\hat{Q}_{2m}^H, \hat{Q}_{2p}^V)$. This link is the same as the link $\hat{L}_o(\hat{Q}_{2p}^H, \hat{Q}_{2m}^V)$ where m and p have been interchanged. For the invariant for this link, we can write

$$\sum_{\ell=0}^n \hat{\mu}_\ell(\hat{Q}_{2m}^H) \sqrt{[2\ell+1]} q^{p\ell(\ell+1)} = \sum_{\ell=0}^n \hat{\mu}_\ell(\hat{Q}_{2p}^H) \sqrt{[2\ell+1]} q^{m\ell(\ell+1)}$$

where we have substituted for $\hat{\mu}_\ell(\hat{Q}_{2p}^V)$ and $\hat{\mu}_\ell(\hat{Q}_{2m}^V)$ on the two sides of this equation from (6.4). Now if we substitute for $\hat{\mu}_\ell(\hat{Q}_{2m}^H)$ and $\hat{\mu}_\ell(\hat{Q}_{2p}^H)$ also and since this relation is valid for arbitrary m and p , we have

$$a_{i\ell} = a_{\ell i} \quad (6.6)$$

Thus this matrix is symmetric and orthogonal. Further in the link in Fig.13b if we take $p=0$, $\hat{L}_o(\hat{Q}_m^H, \hat{Q}_o^V)$ is simply an unknot for any value of m . This implies

$$\sum_{\ell=0}^n \hat{\mu}_\ell(\hat{Q}_{2m}^H) \sqrt{[2\ell+1]} = [n+1]$$

Substitute for $\hat{\mu}_\ell(\hat{Q}_{2m}^H)$ and equate coefficients of various powers of q^m . This leads to

$$\sum_{\ell=0}^n \sqrt{[2\ell+1]} a_{\ell j} = [n+1] \delta_{jo} \quad (6.7)$$

Next we consider the link $L_o(Q_{2p+1}^H, Q_{2m+1}^H)$ obtained by composing two balls containing the rooms Q_{2p+1}^H and Q_{2m+1}^H respectively as shown in Fig 14a. This link is the same as the link $\hat{\mathcal{L}}_{2m+2p+2}$ obtained as the closure of the braid with two oppositely oriented strands with $2m + 2p + 2$ half-twists. Hence its link invariant can be written as

$$\sum_{\ell=0}^n \mu_{\ell}(Q_{2p+1}^H) \mu_{\ell}(Q_{2m+1}^H) = \sum_{\ell=0}^n q^{(p+m+1)\ell(\ell+1)} [2\ell + 1]$$

Here we substitute from Eqn(6.3) for $\mu(Q_{2p+1}^H)$ and $\mu(Q_{2m+1}^H)$ and then equate coefficients of $q^{pi(i+1)}$, $q^{mj(j+1)}$ and $q^{(p+m)\ell(\ell+1)}$ for various values of i, j, ℓ . Thus we obtain again the orthogonality condition (6.5) for the matrix $a_{j\ell}$. Similarly, the links $L_o(Q_{\pm 1}^H, Q_m^V)$ obtained by glueing the two balls containing the rooms $Q_{\pm 1}^H$ and Q_m^V respectively as shown in Fig 14b, are the same as the links $\mathcal{L}_{m\pm 1}$ obtained by the closure of braids with two parallelly oriented strands with $m \pm 1$ half-twists for which link invariants are given by Theorem 6.

Thus

$$\sum_{\ell=0}^n \mu_{\ell}(Q_{\pm 1}^H) (-)^{m(n-\ell)} q^{\frac{m}{2}(n(n+2)-\ell(\ell+1))} [2\ell + 1] = \sum_{\ell=0}^n [2\ell + 1] (-)^{(m\pm 1)(n-\ell)} q^{\frac{(m\pm 1)}{2}(n(n+2)-\ell(\ell+1))}$$

Here substitute from Eqn(6.3) for $\mu_{\ell}(Q_{\pm 1}^H)$. This yields

$$\sum_{j=0}^n \sqrt{[2j + 1]} (-)^j q^{\pm \frac{j(j+1)}{2}} a_{j\ell} = \sqrt{[2\ell + 1]} (-)^{n-\ell} q^{\pm \frac{1}{2}(n(n+2)-\ell(\ell+1))} \quad (6.8)$$

Same equation would emerge if we had considered instead the link $L_o(Q_{2p+1}^V, Q_{\pm 1}^V) \equiv \hat{\mathcal{L}}_{2p+2}, \hat{\mathcal{L}}_{2p}$ obtained by composing two balls containing the rooms Q_{2p+1}^H and $Q_{\pm 1}^V$ respectively.

The matrix $a_{j\ell}$ satisfying conditions (6.5) - (6.8) is given in terms of quantum Racah coefficients for $SU(2)^{11-13}$

$$a_{j\ell} = (-)^{\ell+j-n} \sqrt{[2j + 1][2\ell + 1]} \begin{pmatrix} n/2 & n/2 & j \\ n/2 & n/2 & \ell \end{pmatrix} \quad (6.9)$$

where the quantum Racah coefficients are as given in Appendix A. We have also presented some useful formulae for the Racah coefficients and the matrix $a_{j\ell}$ in this Appendix.

The fact that the matrix $a_{j\ell}$ relating the two bases is the quantum Racah coefficient is not surprising. The two bases referring to the side two strands and the middle two strands attached to the four-punctured S^2 's forming the boundaries of various balls considered above are related by duality of the conformal blocks for four-point correlations of the corresponding $SU(2)_k$ Wess-Zumino conformal field theory on S^2 . The duality matrix for these is indeed given by the quantum Racah coefficients¹³.

It is clear that the Theorems 8 and 9 with the duality matrix $a_{j\ell}$ given by Eqn.(6.9) can be used to construct a variety of link invariants. We can also use these theorems for $n = 1$ to rederive in the present framework many of the results obtained for Jones polynomial. As an example we shall present a new proof of the generalization of the numerator-denominator theorem of Conway for the Jones polynomials derived by Lickorish and Millet in ref.16 within the present framework in Appendix B.

7. Building Blocks for Link Invariants

Although the results in Theorems 8 and 9 do allow us to write down the link invariants for a class of links, these are not enough to study the invariants for arbitrary links. Now we shall attempt to develop several other building blocks which will be useful in obtaining link invariants for an arbitrary link. For this, consider the three - manifold S^3 from which several three-balls (say their number is r) have been removed. This yields a three-manifold with r boundaries, each an S^2 . Wilson lines are placed inside this manifold such that each boundary S^2 is punctured in four places, two ingoing and outgoing. The normalized functional integral over such a manifold defines an operator in the tensor product of Hilbert spaces, $\mathcal{H}^{(1)} \otimes \mathcal{H}^{(2)} \otimes \dots \otimes \mathcal{H}^{(r)}$ where \mathcal{H}^i is the $(n + 1)$ dimensional Hilbert space associated with the i th boundary. This operator can be expanded in terms of a convenient set of basis vectors corresponding to each of these Hilbert spaces.

For example, we have already argued that for a ball with boundary as a four-punctured S^2 , and Wilson lines as shown in Fig.15a, the normalised functional integral is

$$(Fig.15a) = \sum_{\ell=0}^n \sqrt{[2\ell + 1]} | \hat{\phi}_\ell^{(1)} \rangle \quad (7.1)$$

Here the functional integral is multiplied by normalization $N^{-1/2}$ with N as the functional integral over boundaryless empty S^3 . The basis $| \hat{\phi}_\ell^{(1)} \rangle$ of the $(n+1)$ dimensional Hilbert space $\mathcal{H}^{(1)}$ associated with the boundary in terms of which above expansion has been made refers to the middle two (oppositely oriented) strands. The half-twist matrix operating on these strands is diagonal in this basis with eigenvalues given by (5.10). The signature $\epsilon = +$ refers to the orientation of the boundary. For opposite orientation, $\epsilon = -$, we expand in terms of the corresponding basis $\langle \hat{\phi}^{(1)\ell} |$ of the associated dual vector space $\overline{\mathcal{H}}^{(1)}$. Thus the normalised functional integral over the manifold in Fig.15b is

$$(Fig.15b) = \sum_{\ell=0}^n \sqrt{[2\ell + 1]} \langle \hat{\phi}^{(1)\ell} | \quad (7.2)$$

In contrast, the normalized functional integral over the ball with the structure shown in Fig.16a is:

$$\hat{\nu}_1 = \sum_{j,\ell=0}^n \sqrt{[2\ell + 1][2j + 1]} a_{\ell j} | \hat{\phi}_j^{(1)} \rangle = [n + 1] | \hat{\phi}_0^{(1)} \rangle \quad (7.3)$$

Next, let us consider a three-manifold with two boundaries, each a four-punctured S^2 , with four Wilson lines connecting them as indicated in Fig.16b. The normalized functional integral over this manifold can be expanded in terms of the complete set of vectors $| \hat{\phi}_\ell^{(1)} \rangle$ and $| \hat{\phi}_\ell^{(2)} \rangle$ (referring to the middle two strands in both cases) in the Hilbert spaces $\mathcal{H}^{(1)}$

and $\mathcal{H}^{(2)}$ associated with the two boundaries :

$$\hat{\nu}_2 = \sum_{i,j=0}^n \hat{A}_{ij} |\hat{\phi}_i^{(1)}\rangle |\hat{\phi}_j^{(2)}\rangle \quad (7.4)$$

Similarly for the manifold with three boundaries as shown in Fig.16c, each a four-punctured S^2 , we expand in terms of the bases $|\hat{\phi}_\ell^{(1)}\rangle, |\hat{\phi}_\ell^{(2)}\rangle, |\hat{\phi}_\ell^{(3)}\rangle$ of the three Hilbert spaces $\mathcal{H}^{(1)}, \mathcal{H}^{(2)}, \mathcal{H}^{(3)}$ associated with these boundaries and referring to the inner two strands in each case :

$$\hat{\nu}_3 = \sum_{ij\ell}^n \hat{A}_{ij\ell} |\hat{\phi}_i^{(1)}\rangle |\hat{\phi}_j^{(2)}\rangle |\hat{\phi}_\ell^{(3)}\rangle \quad (7.5)$$

Here $\hat{\nu}_3$ represents the functional integral normalized by multiplying with $N^{1/2}$ where N is the functional integral over the empty S^3 .

Now in Eqn.(7.4), the matrix-element \hat{A}_{ij} has to be δ_{ij} . This is obvious, because glueing the manifold shown in Fig.16b onto the manifolds in Figs.16a-c along an S^2 does not change any of these manifolds. That is, this functional integral (7.4) is an identity operator. On the other hand comparing the manifold in (7.5) with those in (7.2) - (7.4) allows us to conclude that $\hat{A}_{ij\ell} = \sum_m a_{im} a_{jm} a_{\ell m} / \sqrt{[2m+1]}$ where a_{im} is the duality matrix. Now glueing two manifolds of the type in Fig.16c(Eqn.7.5) with three boundaries along one each boundary with opposite orientations, would yield a manifold with four boundaries. Repeating this composition several times then yields the following theorem :

Theorem 10: The normalized functional integral for a manifold with r boundaries, each an S^2 , with Wilson lines as indicated in Fig.17 expanded in terms of the bases $|\hat{\phi}_\ell^{(j)}\rangle$ of the Hilbert spaces $\mathcal{H}^{(j)}, j = 1, 2 \dots r$ associated with the boundaries referring to the

middle two strands in each case, is

$$\hat{\nu}_r = \sum_{t=0}^n \frac{\prod_{j=1}^r a_{\ell_j t}}{(\sqrt{[2t+1]})^{r-2}} | \hat{\phi}_{\ell_j}^{(j)} \rangle \quad (7.6)$$

Here the functional integral is normalised by multiplying it by a factor $(N^{1/2})^{r-2}$, where N is the functional integral over boundaryless empty S^3 .

This functional integral may be acted upon by matrix $\hat{B}_{(j)}$, $j = 1, 2 \dots r$ which introduces half-twists in the central two strands of j th boundary :

$$\hat{B}_{(j)} | \hat{\phi}_{\ell}^{(j)} \rangle = (-)^{\ell} q^{\frac{\ell(\ell+1)}{2}} | \hat{\phi}_{\ell}^{(j)} \rangle \quad (7.7)$$

This matrix when operated m_j times then will introduce m_j half-twists in the central two anti-parallel strands of the j th boundary leading to factor $(-)^{m_j \ell_j} q^{m_j \ell_j (\ell_j + 1)/2}$ inside the summation on the right hand side of Eqn.7.6. On the other hand if we operate by the braiding matrix $\hat{B}'_{(j)}$ which introduce half-twists in the first two (or similarly in the last two) strands (again oppositely oriented) of the j th boundary, then

$$(\hat{B}'_{(j)})^{m_j} | \hat{\phi}_{\ell}^{(j)} \rangle = \sum_{s=0}^n (-)^{s m_j} q^{m_j s(s+1)/2} a_{\ell s} a_{s r} | \hat{\phi}_r^{(j)} \rangle \quad (7.8)$$

This way a whole variety of half-twists can be introduced in the diagram in Fig.17 corresponding to Eqn.(7.6). And then composing the resultant manifold with functional integrals of the type in Eqns.(7.1-3) would lead to various link invariants.

In Eqn.(7.6), we have expanded the functional integral with respect to the basis referring to the middle two strands on each of the boundary. The expansion with respect to the basis referring to the first two strands (or equivalently the last two strands) is obtained by recognising that $\sum_{\ell=0}^n a_{\ell t} | \hat{\phi}_{\ell}^{(j)} \rangle$, $t = 0, 1, \dots n$ form such a basis for each of the boundary. Furthermore, the normalized (by factor $(N^{1/2})^{r-2}$) functional integral with orientation on the Wilson lines different from what are given in Fig.17 can also be

obtained in the same manner. For example, the normalized functional integral for the manifold with r -boundaries, each an S^2 , with Wilson lines as indicated in Fig.18 is given by:

$$\nu_r = \sum_{\ell=0}^n \frac{|\phi_\ell^{(1)}\rangle |\phi_\ell^{(2)}\rangle \cdots |\phi_\ell^{(r)}\rangle}{\left(\sqrt{[2\ell+1]}\right)^{r-2}} \quad (7.9)$$

where we have now expanded this functional integral with respect to the basis referring to the first two parallelly oriented strands (or equivalently the last two strands) on each of the boundaries. Again, here this functional integral is multiplied by normalization $(N^{1/2})^{r-2}$. Now the half-twists in the first two strands of the j th boundary which have the same orientation are introduced through the matrix $B_{(j)}, j = 1, 2, \dots, r$ with

$$B_{(j)} |\phi_\ell^{(j)}\rangle = (-)^{n-\ell} q^{\frac{1}{2}(n(n+2)-\ell(\ell+1))} |\phi_\ell^{(j)}\rangle \quad (7.10)$$

so that m_j half-twists would mean a factor $(-)^{m_j(n-\ell)} q^{\frac{m_j}{2}(n(n+2)-\ell(\ell+1))}$ inside the summation in the right-hand side of Eqn.(7.9). The m_j half-twists in the last two strands (again parallelly oriented) also introduce the same factor because $|\phi_\ell^{(j)}\rangle$ are also eigen-vectors with the same eigenvalues of the braid matrix for these two strands. On the other hand for m_j half-twists in the middle two strands (which are oppositely oriented) of the j th boundary are introduced through the braid matrix $B'_{(j)}$:

$$(B'_{(j)})^{m_j} |\phi_\ell^{(j)}\rangle = \sum_{s=0}^n (-)^{m_j s} q^{m_j \frac{s(s+1)}{2}} a_{\ell s} a_{s r} |\phi_r^{(j)}\rangle \quad (7.11)$$

Using the method described here, the functional integral over various three-manifolds containing Wilson lines can be constructed. As another example, the normalized functional integral over the manifold as indicated in Fig.19 containing $2r + 2$ boundaries, $r = 0, 1, 2, \dots$ can be expanded as :

$$(Fig.19) = \left(\frac{1}{[n+1]}\right)^r \sum_{i_\ell=0}^n |\phi_{i_1}^{(1)}\rangle |\phi_{i_1}^{(2)}\rangle \bullet |\phi_{i_2}^{(3)}\rangle |\phi_{i_2}^{(4)}\rangle \bullet \cdots |\phi_{i_{r+1}}^{(2r+1)}\rangle |\phi_{i_{r+1}}^{(2r+2)}\rangle \quad (7.12)$$

Here $|\phi_\ell^{(j)}\rangle$ are the basis of the Hilbert space $\mathcal{H}^{(j)}$ associated with the j th boundary and referring to the first two strands or equivalently the last two strands (oriented in the same direction) attached to that boundary.

It should be noted that in construction of all these functional integral that half-twists are to be introduced in the strands attached to a four-punctured S^2 though braid matrices which have eigenvalues $(-)^{n-\ell}q^{\frac{1}{2}(n(n+2)-\ell(\ell+1))}$, $\ell = 0, 1, \dots, n$ if the strands are oriented in the same direction and $(-)^{\ell}q^{\frac{1}{2}\ell(\ell+1)}$, $\ell = 0, 1, \dots, n$ if the strands are oriented in opposite directions. A number of useful building blocks can be constructed in this manner which then readily yield the link invariants by appropriate composing of the three-manifolds. In Appendix C, we have listed some of these building blocks for reference. They have been used to calculate the knot invariants discussed in the next section.

The method described above can further be generalized to obtain building blocks representing normalized functional integrals over three manifolds with S^2 boundaries which are punctured by Wilson lines at 6,8,10 ... points. The dimensionality of the Hilbert spaces associated with such boundaries is again given by the number of conformal blocks of 6-point, 8-point, 10-point, correlators of the associated $SU(2)_k$ Wess - Zumino model on these boundaries. The duality matrix relating different bases of each of these Hilbert spaces associated with S^2 boundaries punctured at $2m+2$ points with $m = 0, 1, \dots$ are given in terms of quantum 6mj symbols.

8. Explicit Calculation of Knot Invariants

Here we shall present the knot invariants for some knots calculated from the building blocks listed in Appendix C as illustrations. It is possible to obtain the invariants for all the knots and links listed in, for example, Rolfsen's book or the book by Burde and

Zieschang¹⁸. However below we shall list the answers only for knots upto seven crossing number. For a knot these invariants are unchanged if its orientation is reversed. For the mirror reflected knot the invariants are given by the conjugate expressions obtained by replacing q by q^{-1} .

The invariants $V_n[L]$ for knots with seven crossing number listed in Fig.20 are given by

$$\begin{aligned}
0_1 : V_n &= [n + 1] \\
3_1 : V_n &= \sum_{\ell=0}^n [2\ell + 1] (-)^{(n-\ell)} q^{-\frac{3}{2}(n(n+2)-\ell(\ell+1))} \\
4_1 : V_n &= \sum_{\ell,j=0}^n \sqrt{[2j + 1][2\ell + 1]} a_{j\ell} q^{\ell(\ell+1)-j(j+1)} \\
5_1 : V_n &= \sum_{\ell=0}^n [2\ell + 1] (-)^{n-\ell} q^{\frac{5}{2}(n(n+2)-\ell(\ell+1))} \\
5_2 : V_n &= \sum_{j,\ell=0}^n \sqrt{[2j + 1][2\ell + 1]} a_{j\ell} (-)^j q^{n(n+2)-\ell(\ell+1)+\frac{3}{2}j(j+1)} \\
6_1 : V_n &= \sum_{j,\ell=0}^n \sqrt{[2j + 1][2\ell + 1]} a_{j\ell} q^{\ell(\ell+1)-2j(j+1)} \\
6_2 : V_n &= \sum_{i,j,\ell=0}^n \sqrt{[2i + 1][2j + 1]} a_{i\ell} a_{j\ell} (-)^{n-\ell-j} q^{-\frac{3}{2}(n(n+2)-j(j+1))-\frac{\ell(\ell+1)}{2}+i(i+1)} \\
6_3 : V_n &= \sum_{j,\ell,r,s}^n \sqrt{[2j + 1][2s + 1]} a_{j\ell} a_{r\ell} a_{rs} (-)^{\ell+r} q^{-j(j+1)+s(s+1)+\frac{\ell(\ell+1)}{2}-\frac{r(r+1)}{2}} \\
7_1 : V_n &= \sum_{\ell=0}^n [2\ell + 1] (-)^{n-\ell} q^{-\frac{7}{2}(n(n+2)-\ell(\ell+1))} \\
7_2 : V_n &= \sum_{j,\ell=0}^n \sqrt{[2j + 1][2\ell + 1]} a_{j\ell} (-)^j q^{-n(n+2)+\ell(\ell+1)-\frac{5}{2}j(j+1)} \\
7_3 : V_n &= \sum_{j,\ell=0}^n \sqrt{[2j + 1][2\ell + 1]} a_{j\ell} (-)^j q^{\frac{3}{2}j(j+1)+2n(n+2)-2\ell(\ell+1)} \\
7_4 : V_n &= \sum_{j,\ell,r}^n \sqrt{[2j + 1][2r + 1]} a_{j\ell} a_{r\ell} (-)^{n-j-\ell-r} q^{\frac{n(n+2)}{2}-\frac{\ell(\ell+1)}{2}+\frac{3}{2}j(j+1)+\frac{3}{2}r(r+1)}
\end{aligned}$$

$$\begin{aligned}
7_5 : V_n &= \sum_{ij\ell}^n \sqrt{[2i+1][2j+1]} a_{\ell i} a_{\ell j} (-)^{n-j} q^{-\frac{5}{2}n(n+2) + \frac{3}{2}j(j+1) + i(i+1) - \ell(\ell+1)} \\
7_6 : V_n &= \sum_{j\ell r s}^n \sqrt{[2j+1][2s+1]} a_{j\ell} a_{\ell r} a_{r s} (-)^\ell q^{-n(n+2) + j(j+1) - \frac{\ell(\ell+1)}{2} + r(r+1) - s(s+1)} \\
7_7 : V_n &= \sum_{j\ell r s p}^n \sqrt{[2j+1][2p+1]} a_{j\ell} a_{\ell s} a_{s r} a_{r p} (-)^{n-r-s-\ell} q^{-\frac{n(n+2)}{2} + j(j+1) - \frac{\ell(\ell+1)}{2} - \frac{r(r+1)}{2} + \frac{s(s+1)}{2}}
\end{aligned}$$

Here $a_{j\ell}$ is the duality matrix given in Appendix A.

Using the building blocks for normalized functional integrals over three manifolds with 4 and higher punctures on their S^2 boundaries, the above calculations can be extended to obtain the invariants for the whole tables of knots and links given in ref.17 in a straight forward manner.

Using the explicit representation for the duality matrix a_{jl} for $n = 1$ as given in Appendix A, the above expressions can easily be seen to yield the Jones one-variable polynomials² for these knots. On the other hand, with the help of explicit representation for a_{jl} for $n = 2$ as given in Appendix A, we obtain the polynomials¹⁹ calculated explicitly by Akutsu, Deguchi and Wadati from the three-state exactly solvable model¹⁰.

9. Concluding Remarks

Following Witten⁴, here we have studied the $SU(2)$ Chern-Simons theory in three dimensions as a theory of knots and links. A systematic method has been developed to obtain link invariants. The relation of a Chern-Simons theory on three-manifold with boundary to the Wess-Zumino conformal field theory on the boundary has been exploited in doing so. Expectation value of Wilson link operators with the same spin $n/2$ representation of $SU(2)$ living on each of the component knots of the link yields a whole variety of link invariants. The Jones one variable polynomial corresponds to $n = 1$. For higher n ,

these are the new link invariants discussed by Wadati, Deguchi and Akutsu from the point of view of $N = n + 1$ state exactly solvable statistical models¹⁰. As illustration of our method we have also computed explicitly these invariants for knots upto seven crossing points. The method can be generalized to links where different representations of $SU(2)$ are placed on the component knots. Such links may be called multicoloured. Expectation values of Wilson link operators associated with such multicoloured links would then provide new link invariants. The knowledge of the expectation value of Wilson operators for any link with arbitrary representations of the gauge group living on the component knots would then provide a complete solution of the non-abelian Chern-Simons theory in three dimensions. A detailed discussion of this will be presented elsewhere.

Generalization of our discussion to an arbitrary compact gauge group, say $SU(N)$, is rather straight forward. We shall take up this elsewhere.

Acknowledgements

We thank R.Jagannathan and K.Srinivasa Rao for discussions on quantum Racah coefficients.

Appendix A

Here we shall list some useful properties of the quantum Racah coefficients and the duality matrix $a_{j\ell}$.

The quantum Racah coefficients are given by ¹¹⁻¹³

$$\begin{aligned}
\begin{pmatrix} j_1 & j_2 & j_{12} \\ j_3 & j_4 & j_{23} \end{pmatrix} &= \Delta(j_1, j_2, j_{12})\Delta(j_3, j_4, j_{12})\Delta(j_1, j_4, j_{23})\Delta(j_3, j_2, j_{23}) \\
&\sum_{m \geq 0} (-)^m [m+1]! \{ [m - j_1 - j_2 - j_{12}]! \\
&[m - j_3 - j_4 - j_{12}]! [m - j_1 - j_4 - j_{23}]! \\
&[m - j_3 - j_2 - j_{23}]! [j_1 + j_2 + j_3 + j_4 - m]! \\
&[j_1 + j_3 + j_{12} + j_{23} - m]! [j_2 + j_4 + j_{12} + j_{23} - m]! \}^{-1} \quad (A.1)
\end{aligned}$$

and

$$\Delta(a, b, c) = \sqrt{\frac{[-a+b+c]![a-b+c]![a+b-c]!}{[a+b+c+1]!}} \quad (A.2)$$

Here $[a]! = [a][a-1][a-2]\dots[2][1]$. The $SU(2)$ spins are related as $\vec{j}_1 + \vec{j}_2 + \vec{j}_3 = \vec{j}_4$, $\vec{j}_1 + \vec{j}_2 = \vec{j}_{12}$, $\vec{j}_2 + \vec{j}_3 = \vec{j}_{23}$

The duality matrix $a_{j\ell}$ where three spins, each $n/2$ is combined into spin $n/2$ is given by

$$a_{j\ell} = (-)^{\ell+j-n} \sqrt{[2j+1][2\ell+1]} \begin{pmatrix} n/2 & n/2 & j \\ n/2 & n/2 & \ell \end{pmatrix} \quad (A.3)$$

The q -Racah coefficients satisfy the following properties¹¹ :

$$\begin{pmatrix} j_1 & j_2 & j \\ j_3 & j_4 & \ell \end{pmatrix} = \begin{pmatrix} j_1 & j_4 & \ell \\ j_3 & j_2 & j \end{pmatrix} \quad (A.4)$$

$$\begin{pmatrix} j_1 & j_2 & 0 \\ j_3 & j_4 & \ell \end{pmatrix} = \frac{(-1)^{\ell+j_2+j_3} \delta_{j_1 j_2} \delta_{j_3 j_4}}{\sqrt{[2j_2+1][2j_3+1]}} \quad (A.5)$$

$$\sum_j [2j+1][2\ell+1] \begin{pmatrix} j_1 & j_2 & j \\ j_3 & j_4 & \ell \end{pmatrix} \begin{pmatrix} j_1 & j_2 & j \\ j_3 & j_4 & \ell' \end{pmatrix} = \delta_{\ell\ell'} \quad (A.6)$$

$$\begin{aligned}
\sum_x (-)^{j+\ell+x} [2x+1] q^{-C_x} \begin{pmatrix} j_1 & j_2 & x \\ j_3 & j_4 & j \end{pmatrix} \begin{pmatrix} j_1 & j_2 & x \\ j_4 & j_3 & \ell \end{pmatrix} = \\
\begin{pmatrix} j_1 & j_3 & j \\ j_2 & j_4 & \ell \end{pmatrix} q^{C_j/2+C_\ell/2} q^{-C_{j_1}/2-C_{j_2}/2-C_{j_3}/2-C_{j_4}/2} \quad (A.7)
\end{aligned}$$

where $C_j = j(j+1)$ is the Casimir invariant in the spin j representation R_{2j} . These relations respectively imply the following properties for the duality matrix $a_{j\ell}$ defined in (A.3)

$$a_{j\ell} = a_{\ell j} \quad (A.8)$$

$$a_{j0} = \frac{\sqrt{[2j+1]}}{[n+1]} \quad (A.9)$$

$$\sum_{\ell=0}^n a_{\ell i} a_{\ell j} = \delta_{ij} \quad (A.10)$$

$$\sum_x (-)^{n-x} q^{\pm \frac{1}{2}(n(n+2)-x(x+1))} a_{jx} a_{\ell x} = (-)^{j+\ell} q^{\pm(j(j+1)+\ell(\ell+1))/2} a_{j\ell} \quad (A.11)$$

Further notice that (A.9) and (A.10) imply:

$$\sum_{\ell=0}^n \sqrt{[2\ell+1]} a_{\ell j} = \delta_{j0} [n+1] \quad (A.12)$$

and (A.9) and (A.11) imply :

$$\sum_{j=0}^n \sqrt{[2j+1]} (-)^j q^{\pm \frac{j(j+1)}{2}} a_{jl} = (-)^{n-l} \sqrt{[2\ell+1]} q^{\pm \frac{1}{2}(n(n+2)-\ell(\ell+1))} \quad (A.13)$$

Also (A.10) and (A.11) imply:

$$\sum_{r,s} (-)^{r+s} q^{\pm(\frac{r(r+1)}{2} + \frac{s(s+1)}{2})} a_{\ell r} a_{rs} a_{sj} = \delta_{\ell j} (-)^{n-\ell} q^{\pm(\frac{n(n+1)}{2} + \frac{\ell(\ell+1)}{2})} \quad (A.14)$$

Another useful relation is

$$\sum_{r,s} \sqrt{[2r+1][2s+1]} a_{rs} q^{r(r+1)+s(s+1)} = \sum [2\ell+1] (-)^{\ell} q^{\frac{3}{2}\ell(\ell+1)} \quad (A.15)$$

It is instructive to write down this duality matrix $a_{j\ell}$ explicitly for various low values of n . We need this to compare the results obtained here with those of Jones² and Akutsu, Deguchi and Wadati¹⁰ for the link invariants for $n = 1$ and $n = 2$ respectively. The duality matrix for these two values of n reads :

(i) $\mathbf{n} = \mathbf{1}$

$$a_{j\ell} = \frac{1}{[2]} \begin{pmatrix} 1 & \sqrt{[3]} \\ \sqrt{[3]} & -1 \end{pmatrix} \quad (\text{A.16})$$

(ii) $\mathbf{n} = 2$

$$a_{j\ell} = \frac{1}{[3]} \begin{pmatrix} 1 & \sqrt{[3]} & \sqrt{[5]} \\ \sqrt{[3]} & \frac{[3]([5]-1)}{[4][2]} & -\frac{[2]\sqrt{[5][3]}}{[4]} \\ \sqrt{[5]} & -\frac{[2]\sqrt{[5][3]}}{[4]} & \frac{[2]}{[4]} \end{pmatrix} \quad (A.17)$$

Appendix B

Here we shall illustrate by an example how the framework developed in this paper can be used to rederive many of the results already known for Jones polynomials.

The generalization of numerator-denominator theorem of Conway for Jones polynomials has been proved by Lickorish and Millet¹⁶. We shall present a new proof for this theorem here .

Theorem : For the links depicted in Fig.21,this theorem states that

$$\begin{aligned} \cup(\cup^2 - 1)\hat{L}_o(\hat{A}, \hat{B}) &= \cup\{\hat{L}_o(\hat{A}, \hat{Q}_o^H)\hat{L}_o(\hat{Q}_o^H, \hat{B}) + \hat{L}_o(\hat{A}, \hat{Q}_o^V)\hat{L}_o(\hat{Q}_o^V, \hat{B})\} \\ &\quad - \{\hat{L}_o(\hat{A}, \hat{Q}_o^H)\hat{L}_o(\hat{Q}_o^V, \hat{B}) + \hat{L}_o(\hat{A}, \hat{Q}_o^V)\hat{L}_o(\hat{Q}_o^H, \hat{B})\} \end{aligned} \quad (B.1)$$

where the symbol for each of the link diagrams itself represents the Jones link invariant $V_1[L]$.

The proof of this theorem is rather straight forward in our framework. We write the link invariants above as :

$$\hat{L}_o(\hat{A}, \hat{B}) = \hat{\mu}_o(\hat{A})\hat{\mu}_o(\hat{B}) + \hat{\mu}_1(\hat{A})\hat{\mu}_1(\hat{B}) \quad (B.2)$$

$$\hat{L}_o(\hat{Q}_o^V, \hat{B}) = \hat{\mu}_o(\hat{B}) + \sqrt{[3]} \hat{\mu}_1(\hat{B}) \quad (B.3)$$

$$\hat{L}_o(\hat{Q}_o^H, \hat{B}) = \hat{\mu}_o(\hat{B}) [2] \quad (B.4)$$

$$\hat{L}_o(\hat{A}, \hat{Q}_o^V) = \hat{\mu}_o(\hat{A}) + \sqrt{[3]} \hat{\mu}_1(\hat{A}) \quad (B.5)$$

$$\hat{L}_o(\hat{A}, \hat{Q}_o^H) = \hat{\mu}_o(\hat{A}) [2] \quad (B.6)$$

where we have used from Theorem 9.

$$\hat{\mu}_\ell(\hat{Q}_o^V) = \sqrt{[2\ell + 1]}, \quad \hat{\mu}_\ell(\hat{Q}_o^H) = \sum_{j=0}^n \sqrt{[2j + 1]} a_{j\ell} = \delta_{\ell o}[n + 1]$$

Now if we solve for $\hat{\mu}_\ell(\hat{A})$ and $\hat{\mu}_\ell(\hat{B})$, $\ell = 0, 1$ from Eqns(B.3-B.6), we have

$$\begin{aligned} \hat{\mu}_o(\hat{X}) &= \cup \hat{L}_o(\hat{Q}_0^H, \hat{B}) \\ \hat{\mu}_1(\hat{X}) &= \frac{\cup \hat{L}_o(\hat{X}, \hat{Q}_0^V) - \hat{L}_o(\hat{X}, \hat{Q}_0^H)}{\cup \sqrt{(\cup^2 - 1)}} \end{aligned} \quad (B.7)$$

where $\hat{X} = \hat{A}, \hat{B}$ and the link invariant for the unknot ($n = 1$) $\cup = [2]$ and $[3] = \cup^2 - 1$. Substituting these values (B.7) into (B.2) then, immediately yields the theorem above.

Appendix C

In the following, we list various normalized functional integrals expanded in terms of the bases vectors referring to the middle two of the four strands attached to each of the boundaries , S^2 . The diagram for the manifold itself will represent the normalised functional integral. In the following numbers on the left hand side refer to the diagrams in Fig.22, respectively:

$$(1) = \sum_{\ell=0}^n \sqrt{[2\ell + 1]} | \hat{\phi}_\ell^{(1)} \rangle$$

$$(2) = [n + 1] | \hat{\phi}_o^{(1)} \rangle$$

$$\begin{aligned}
(3) &= \sum_{\ell=0}^n \sqrt{[2\ell+1]} q^{m\ell(\ell+1)} | \hat{\phi}_\ell^{(1)} \rangle, \\
(4) &= \sum_{\ell=0}^n \sqrt{[2\ell+1]} (-1)^\ell q^{\frac{2m+1}{2}\ell(\ell+1)} | \hat{\phi}_\ell^{(1)} \rangle \\
(5) &= \sum_{j,\ell=0}^n \sqrt{[2j+1]} a_{j\ell} q^{mj(j+1)} | \hat{\phi}_\ell^{(1)} \rangle, \\
(6) &= \sum_{j\ell}^n \sqrt{[2j+1]} a_{j\ell} (-1)^j q^{\frac{2m+1}{2}j(j+1)} | \hat{\phi}_\ell^{(1)} \rangle \\
(7) &= \sum_j q^{mj(j+1)} | \hat{\phi}_j^{(1)} \rangle | \hat{\phi}_j^{(2)} \rangle \\
(8) &= \sum_{j=0}^n (-1)^j q^{\frac{2m+1}{2}j(j+1)} | \hat{\phi}_j^{(1)} \rangle | \hat{\phi}_j^{(2)} \rangle \\
(9) &= \sum_{j,\ell} \sqrt{\frac{[2\ell+1]}{[2j+1]}} a_{\ell j} q^{m(n(n+2)-\ell(\ell+1))} | \hat{\phi}_j^{(1)} \rangle | \hat{\phi}_j^{(2)} \rangle \\
(10) &= \sum_{j,\ell} \sqrt{\frac{[2\ell+1]}{[2j+1]}} a_{\ell j} q^{m\ell(\ell+1)} | \hat{\phi}_j^{(1)} \rangle | \hat{\phi}_j^{(2)} \rangle \\
(11) &= \sum_{j,\ell=0}^n \sqrt{\frac{[2\ell+1]}{[2j+1]}} a_{\ell j} (-1)^{n-\ell} q^{\frac{2m+1}{2}(n(n+2)-\ell(\ell+1))} | \hat{\phi}_j^{(1)} \rangle | \hat{\phi}_j^{(2)} \rangle \\
(12) &= \sum \sqrt{\frac{[2\ell+1]}{[2j+1]}} a_{\ell j} (-1)^\ell q^{\frac{2m+1}{2}\ell(\ell+1)} | \hat{\phi}_j^{(1)} \rangle | \hat{\phi}_j^{(2)} \rangle \\
(13) &= \sum_{j\ell r} a_{jr} a_{\ell r} q^{(m+p)r(r+1)} | \hat{\phi}_j^{(1)} \rangle | \hat{\phi}_\ell^{(2)} \rangle \\
(14) &= \sum_{j\ell r} a_{jr} a_{\ell r} q^{(m+p+1)r(r+1)} | \hat{\phi}_j^{(1)} \rangle | \hat{\phi}_\ell^{(2)} \rangle \\
(15) &= \sum a_{jr} a_{\ell r} (-1)^r q^{\frac{2m+2p+1}{2}r(r+1)} | \hat{\phi}_j^{(1)} \rangle | \hat{\phi}_\ell^{(2)} \rangle \\
(16) &= \sum_{ij\ell r} \frac{a_{ij} a_{jr} a_{\ell r} \sqrt{[2\ell+1]}}{\sqrt{[2r+1]}} q^{m\ell(\ell+1)} | \hat{\phi}_i^{(1)} \rangle | \hat{\phi}_j^{(2)} \rangle \\
(17) &= \sum_{ij\ell r} \frac{a_{ir} a_{jr} a_{\ell r} \sqrt{[2\ell+1]}}{\sqrt{[2r+1]}} q^{m(n(n+2)-\ell(\ell+1))} | \hat{\phi}_i^{(1)} \rangle | \hat{\phi}_j^{(2)} \rangle \\
(18) &= \sum_{ij\ell r} \frac{a_{ir} a_{jr} a_{\ell r} \sqrt{[2\ell+1]}}{\sqrt{[2r+1]}} (-1)^\ell q^{\frac{2m+1}{2}\ell(\ell+1)} | \hat{\phi}_i^{(1)} \rangle | \hat{\phi}_j^{(2)} \rangle
\end{aligned}$$

$$\begin{aligned}
(19) &= \sum_{ij\ell r} \frac{a_{ir}a_{jr}a_{\ell r}\sqrt{[2\ell+1]}}{\sqrt{[2r+1]}} (-)^{n-\ell} q^{\binom{2m+1}{2}(n(n+2)-\ell(\ell+1))} | \hat{\phi}_i^{(1)} \rangle | \hat{\phi}_j^{(2)} \rangle \\
(20) &= \sum_{ij\ell r s} \frac{a_{ir}a_{jr}a_{\ell r}a_{sr}\sqrt{[2\ell+1][2s+1]}}{[2r+1]} q^{m\ell(\ell+1)} q^{ps(s+1)} | \hat{\phi}_i^{(1)} \rangle | \hat{\phi}_j^{(2)} \rangle \\
(21) &= \sum_{ij\ell r s} \frac{a_{ir}a_{jr}a_{\ell r}a_{sr}}{[2r+1]} \sqrt{[2\ell+1][2s+1]} (-)^{\ell+s} q^{\binom{2m+1}{2}(n(n+2)-\ell(\ell+1))} \\
&\quad \bullet q^{\binom{2p+1}{2}(n(n+2)-s(s+1))} | \hat{\phi}_i^{(1)} \rangle | \hat{\phi}_j^{(2)} \rangle \\
(22) &= \sum_{ij\ell r s} \frac{a_{ir}a_{jr}a_{\ell r}a_{sr}}{[2r+1]} \sqrt{[2\ell+1][2s+1]} q^{m(n(n+2)-\ell(\ell+1))} \\
&\quad \bullet q^{p(n(n+2)-s(s+1))} | \hat{\phi}_i^{(1)} \rangle | \hat{\phi}_j^{(2)} \rangle \\
(23) &= \sum_{ij\ell r s} \frac{a_{ir}a_{jr}a_{\ell r}a_{sr}\sqrt{[2\ell+1][2s+1]}}{[2r+1]} (-)^{\ell+s} q^{\binom{2m+1}{2}\ell(\ell+1)} \\
&\quad \bullet q^{\binom{2p+1}{2}s(s+1)} | \hat{\phi}_i^{(1)} \rangle | \hat{\phi}_j^{(2)} \rangle \\
(24) &= \sum_{j\ell r} a_{rj}a_{r\ell} q^{m(n(n+2)-r(r+1))} | \hat{\phi}_j^{(1)} \rangle | \hat{\phi}_\ell^{(2)} \rangle \tag{C.1}
\end{aligned}$$

Now let us present some functional integrals expanded in terms of the bases vectors referring to the first two strands on the left (and equivalently the last two on the right) attached to the boundaries, each of which is an S^2 with four punctures as shown in Fig.23. For the diagrams listed in this figure, the normalized functional integrals are as follows :

$$\begin{aligned}
(1) &= \sum_{\ell=0}^n \sqrt{[2\ell+1]} | \phi_\ell^{(1)} \rangle, \\
(2) &= \sum_{\ell=0}^n \sqrt{[2\ell+1]} (-)^{m(n-\ell)} q^{\frac{m}{2}(n(n+2)-\ell(\ell+1))} | \phi_\ell^{(1)} \rangle \\
(3) &= \sum_{j,\ell}^n \sqrt{[2j+1]} (-)^j a_{j\ell} q^{\binom{2m+1}{2}j(j+1)} | \phi_\ell^{(1)} \rangle, \\
(4) &= \sum_{j\ell}^n \sqrt{[2j+1]} a_{j\ell} q^{mj(j+1)} | \phi_\ell^{(1)} \rangle
\end{aligned}$$

$$\begin{aligned}
(5) &= \sum_{\ell=0}^n (-)^{(m+p)(n-\ell)} q^{\binom{m+p}{2}(n(n+2)-\ell(\ell+1))} |\phi_\ell^{(1)}\rangle |\phi_\ell^{(2)}\rangle \\
(6) &= \sum_{j\ell} \sqrt{\frac{[2j+1]}{[2\ell+1]}} (-)^j a_{j\ell} q^{\binom{2m+1}{2}j(j+1)} |\phi_\ell^{(1)}\rangle |\phi_\ell^{(2)}\rangle \\
(7) &= \sum_{j\ell} \sqrt{\frac{[2j+1]}{[2\ell+1]}} q^{mj(j+1)} a_{j\ell} |\phi_\ell^{(1)}\rangle |\phi_\ell^{(2)}\rangle \\
(8) &= \sum_{j\ell} \sqrt{\frac{[2j+1]}{[2\ell+1]}} q^{m(n(n+2)-j(j+1))} a_{j\ell} |\phi_\ell^{(1)}\rangle |\phi_\ell^{(2)}\rangle \\
(9) &= \sum_{j\ell} \sqrt{\frac{[2j+1]}{[2\ell+1]}} (-)^{n-j} q^{\binom{2m+1}{2}(n(n+2)-j(j+1))} a_{j\ell} |\phi_\ell^{(1)}\rangle |\phi_\ell^{(2)}\rangle \\
(10) &= \sum_{ij\ell} q^{m\ell(\ell+1)} a_{\ell i} a_{\ell j} |\phi_i^{(1)}\rangle |\phi_j^{(2)}\rangle \\
(11) &= \sum_{ij\ell} (-)^\ell q^{\binom{2m+1}{2}\ell(\ell+1)} a_{\ell i} a_{\ell j} |\phi_i^{(1)}\rangle |\phi_j^{(2)}\rangle \\
(12) &= \sum_{ij\ell r} \frac{a_{ir} a_{jr} a_{\ell r} \sqrt{[2\ell+1]}}{\sqrt{[2r+1]}} q^{m\ell(\ell+1)} |\phi_i^{(1)}\rangle |\phi_j^{(2)}\rangle \\
(13) &= \sum_{ij\ell r} \frac{a_{ir} a_{jr} a_{\ell r} \sqrt{[2\ell+1]}}{\sqrt{[2r+1]}} (-)^\ell q^{\binom{2m+1}{2}\ell(\ell+1)} |\phi_i^{(1)}\rangle |\phi_j^{(2)}\rangle \\
(14) &= \sum_{ij\ell r} \frac{a_{ir} a_{jr} a_{\ell r} \sqrt{[2\ell+1]}}{\sqrt{[2r+1]}} q^{m(n(n+2)-\ell(\ell+1))} |\phi_i^{(1)}\rangle |\phi_j^{(2)}\rangle \\
(15) &= \sum_{ij\ell r} \frac{a_{ir} a_{jr} a_{\ell r} \sqrt{[2\ell+1]}}{\sqrt{[2r+1]}} (-)^{n-\ell} q^{\binom{2m+1}{2}(n(n+2)-\ell(\ell+1))} |\phi_i^{(1)}\rangle |\phi_j^{(2)}\rangle \tag{C.2}
\end{aligned}$$

References

- [1] S.K.Donaldson, J.Diff.Geom. **18** (1983) 269 ; Polynomial invariants for smooth four-manifolds, Oxford preprint.
- [2] V.F.R. Jones, Bull. AMS **12** (1985) 103 ; Ann. of Math. **128** (1987) 335.

- [3] E.Witten, Commun. Math. Phys. **117** (1988) 353.
- [4] E.Witten, Commun. Math. Phys. **121** (1989) 351.
- [5] D.Birmingham, M.Rakowski and G.Thomson, Nucl. Phys. **B315** (1989) 577 ;
L.Baulieu and B.Grossman, Phys. Letts. **B214** (1988) 223 ; R.K.Kaul and
R.Rajaraman, Phys. Letts.**B** (in press).
- [6] M.F.Atiyah in "Oxford Seminar on Jones-Witten Theory", 1988 ; M.F.Atiyah, Publ.
Math. IHES **68** (1988) 175.
- [7] P.Freyd, D.Yetter, J.Hoste, W.B.R.Lickorish, K.Millet and A.Ocneanu, Bull. AMS
12 (1985) 239 ; J.H.Przytycki and K.P.Traczyk, Kobe J.Math. **4** (1987) 115.
- [8] L.Kaufmann, Topology **26** (1987) 395.
- [9] V.G.Turaev, Inv. Math. **92** (1988) 527.
- [10] M.Wadati, T.Deguchi and Y.Akutsu, Phys. Rep. **180** (1989) 247 and references
therein.
- [11] A.N.Kirillov and N.Yu.Reshetikhin, Representation algebra $U_q(SL(2))$, q -orthogonal
polynomials and invariants of links, LOMI preprint E-9-88; See also 'New Develop-
ments in the Theory of Knots', World Scientific Ed.T.Kohno (1989).
- [12] L.Alvarez Gaume, G.Gomez and G.Sierra, Phys. Letts. **B220** (1989) 42.
- [13] For a review see, L.Alvarez Gaume and G.Sierra, CERN preprint TH.5540/89.
- [14] K.Yamagishi, M-L Ge and Y-S Wu, Letts. Math. Phys. **19** (1990) 15.
- [15] R.Kaul and R.Rajaraman, Phys. Letts. **B249** (1990) 433.
- [16] W.B.R.Lickorish and K.C.Millet, Topology **26** (1987) 107.

- [17] G.Moore and N.Seiberg, Lectures on RCFT in "Superstring '89", ed. M.Green et.al., World Scientific, Singapore (1990).
- [18] D.Rolfsen, "Knots and Links", Publish or Perish Inc., Berkely (1976) ; G.Burde and H.Zieschang, "Knots", de Gruyter Studies in Mathematics **5**, Walter de Gruyter, Berlin, New York (1985).
- [19] Our normalization differs from those in Refs.2 and 10, where the invaraint for an unknot is taken to be one. Thus to compare our results for $n = 1$ and $n = 2$ with those of these references, we need to multiply their expressions by $V_n[\cup] = [n + 1]$.

Figure Captions

Fig.[1]. Connected sum of two links L_1, L_2 .

Fig.[2]. Examples of rooms.

Fig.[3]. Composition of two balls B_1, B_2 leads to link $L_m(A)$ in S^3 .

Fig.[4]. Half twists in two strands.

Fig.[5]. Composing of balls B_1 and B_2 gives link $\hat{L}_{2m}(\hat{A})$ in S^3 .


Fig.[6]. Link $\hat{L}_{2m+1}(\hat{A}')$ with room  .

Fig.[7]. Composition of balls B_1 and B_2 yields link $L(A_1, A_2)$ in S^3 .

Fig.[8]. (a) Parallely oriented two-strand braid with m half-twists and
(b) its closure \mathcal{L}_m .

Fig.[9]. Composition of balls B_1 and B_2 yields link $\hat{L}_{2m}(\hat{A}_1, \hat{A}_2)$ in S^3 .

Fig.[10]. (a) Oppositely oriented two-strand braid with $2m$ half-twists and
(b) its closure $\hat{\mathcal{L}}_{2m}$.

Fig.[11]. Rooms Q_m^V and Q_{2p+1}^H .

Fig.[12]. Rooms $\hat{Q}_m^V, \hat{Q}_{2p}^H$ and \hat{Q}_p^H

Fig.[13]. The links (a) $\hat{L}_o(\hat{Q}_{2m}^H, \hat{Q}_{2p}^H) \equiv \hat{\mathcal{L}}_{2m+2p}$ and
 (b) $\hat{L}_o(\hat{Q}_{2m}^H, \hat{Q}_{2p}^V) \equiv \hat{L}_o(\hat{Q}_{2m}^V, \hat{Q}_{2p}^H)$

Fig.[14]. The links (a) $L_o(Q_{2p+1}^H, Q_{2m+1}^H) = \hat{\mathcal{L}}_{2p+2m+2}$ and
 (b) $L_o(Q_1^H, Q_m^V) = \mathcal{L}_{m+1}$

Fig.[15]. Vectors corresponding to Eqns.7.1 and 7.2 respectively.

Fig.[16]. Diagrammatic representations of functional integrals $\hat{\nu}_1, \hat{\nu}_2, \hat{\nu}_3$
 in Eqns.7.3-5 respectively.

Fig.[17]. Functional integral over a manifold with r boundaries $\hat{\nu}_r$ of Eqn.7.6.

Fig.[18]. Functional integral over a manifold with r boundaries ν_r of Eqn.7.9.

Fig.[19]. Functional integral over a manifold with $2r + 2$ boundaries (Eqn.7.12).

Fig.[20]. Knot projections upto seven crossing points.

Fig.[21]. Link diagrams for numerator-denominator theorem (Eqn.B.1).

Fig.[22]. Building blocks corresponding to the Eqns.(C.1) respectively.

Fig.[23].Building blocks corresponding to the Eqns.(C.2) respectively.